International Journal on Science and Technology (IJSAT)
E-ISSN: 2229-7677 ● Website: www.ijsat.org ● Email: editor@ijsat.org

Plant-Mediated Synthesis of Zinc Oxide-Functionalized Carbon Nanocomposites with Improved Antibacterial Performance

Christma Eunice Sherina. P[1], Francis Tisha. N[2], N.S. Nirmala Jothi[3]

[1,2,3]Department of Physics, Loyola College, Chennai

Abstract

Zinc oxide-functionalized carbon (ZnO-C) nanocomposites have gained interest due to their superior antibacterial activity, biocompatibility, and potential for biomedical applications. In the current work, ZnO-C nanocomposites were produced utilizing a simple green solvothermal process with Daucus carota extract as a natural reducing and stabilizing agent and citric acid as a carbon precursor. The nanocomposites were studied by X-ray diffraction, Fourier transform infrared spectroscopy, scanning electron microscopy combined with energy-dispersive X-ray spectroscopy and ultraviolet-visible spectroscopy. The characterisation results proved the effective synthesis of nanocrystalline ZnO-C nanocomposites with distinct structural and functional properties. The antibacterial activity was tested against Pseudomonas aeruginosa, Enterococcus faecalis, methicillin-resistant Staphylococcus aureus (MRSA), and Klebsiella pneumoniae using the agar well diffusion technique. The ZnO-C nanocomposites indicated selective antibacterial action, with enhanced inhibition observed against Pseudomonas aeruginosa (24 mm) and moderate activity against MRSA (11-14 mm). Enterococcus faecalis and Klebsiella pneumoniae showed low susceptibility. Comparative testing with carbon nanoparticles demonstrated that ZnO functionalization improved antibacterial activity against Pseudomonas aeruginosa, revealing the synergistic impact of ZnO nanoparticles with the carbon matrix.

Keywords

Functionalization, Carbon, Zinc oxide, Daucus carota, Solvothermal synthesis, Antibacterial activity

1. Introduction

Metal oxide–functionalized carbon nanocomposites represent one of the major advances in hybrid nanomaterials, combining the properties of metal oxides and carbonaceous materials. The overall performance of these nanocomposites is improved by combining the catalytic, optical, magnetic and antibacterial properties of metal oxides with the large specific surface area, chemical stability, various surface chemistries, and good electron transfer properties of carbon. They have been used in many different areas, including catalysis, energy storage, environmental restoration, biosensing, drug delivery, tissue engineering, and antimicrobial therapy.

Zinc oxide (ZnO) has attracted specific interest because of its wide band gap, high exciton binding energy, chemical stability, biocompatibility and broad-spectrum antibacterial activity [1]. ZnO nanoparticles exhibit antibacterial activity through various mechanisms, including generation of reactive oxygen species (ROS), release of Zn2+ ions and direct interaction with bacterial membranes that leads to cell membrane damage and oxidative stress [2]. However, pure ZnO nanoparticles tend to agglomerate because of their high surface energy [3], which leads to a decrease in antibacterial activity and requires functionalization with carbon materials. This functionalization can improve the dispersion, stability, electron transport and active sites of ZnO and the additional oxygen-containing functional groups can also improve the interactions with bacteria. The shift towards sustainable synthesis of nanomaterials stresses the use of green methodology that negates the use of hazardous chemical reagents and solvents and encourages eco-friendly alternatives. The green synthesis utilises naturally available phytochemicals as agents to reduce, cap and stabilise nanoparticles [4]. Plant extracts are especially beneficial due to their cost-effectiveness, renewability, biodegradability and abundance of bioactive substances that lead to stable and efficient nanostructures. Successful examples of green-synthesised ZnO nanoparticles demonstrate the potential of this method, such as those created from Azadirachta indica [5] and Aloe vera extracts [6], which exhibited improved antibacterial properties. Recent studies even explore the use of different fruit and vegetable extracts as carbon sources [7], [8], [9], [10], demonstrating the potential of these natural materials to produce carbonisation in addition to beneficial surface functionalization.

Daucus carota (carrot) is considered as a promising source of phenolic compounds, carotenoids, flavonoids and other active metabolites [11] which are relevant for eco-friendly nanomaterial synthesis. Its phytochemical composition enables the reduction of metal ions and stabilisation of nanoparticles and the development of functionalized carbon frameworks [12]. Despite the large amount of research on green-synthesized ZnO and carbon-based nanomaterials, there are few studies on ZnO-functionalized carbon nanocomposites derived from Daucus carota. Furthermore, the synergistic effects of phytochemicals on augmenting the antibacterial activity of ZnO NPs have not been well elucidated. This study investigates the fabrication of solvothermal-produced zinc oxide-functionalized carbon nanocomposites. We use Daucus carota extract as a naturally occurring, non-toxic reducing agent, and citric acid is used as a carbon precursor. During the characterisation of the nanocomposites, we investigated their structural, optical, and morphological properties, and conducted rigorous antibacterial activity assessments against relevant Gram-positive and Gram-negative bacteria. We believe this work provides insight into the solvothermal technique of synthesising ZnO – functionalised carbon nanocomposites (ZnO-C) with a higher degree of antibacterial activity for potential future biomedical applications.

2. Experimental

A solvothermal approach, adapted from D'Souza et al. [13] and Yan et al. [14], was used to synthesise zinc oxide-functionalized carbon nanocomposites. The phytochemical reducing agent was fresh Daucus carota (carrot), purchased from neighbourhood farmers' markets in Chennai, Tamil Nadu, India. Citric acid (CA), 1-(2-pyridylazo)-2-naphthol (PAN), ethylenediaminetetraacetic acid (EDTA), and zinc nitrate ($Zn(NO_3)_2$) were procured from Sigma-Aldrich and utilised without purification. In the course of the synthesis, standard double-distilled water (pH = 7) and standard analytically graded chemicals were used.

2.1 Preparation of carrot extract

Freshly picked carrots (about 250 grams) were properly washed with distilled water, then chopped into small chunks and processed to prepare a carrot extract. This extract was solvothermally treated at 120°C for 20 minutes to preserve the bioactive phytochemicals contributing to nanoparticle reduction and stability. Upon natural cooling to ambient room temperature, the extract was filtered, aliquoted, and kept at 4 °C until required.

2.2 Green Synthesis of Carrot Extract-Mediated Zinc Oxide functionalised Carbon Nanocomposites

Carbon nanoparticles were obtained by combining citric acid and PAN indicator (0.05 g) in 50 mL of ethanol with continuous magnetic stirring until a homogeneous solution was achieved. EDTA was then added dropwise to enhance complexation and controlled particle formation, followed by the progressive addition of 70 mL of carrot extract while stirring continuously. The resultant precursor solution was transferred to a Teflon-lined stainless-steel autoclave and heated to 120 °C for 20 minutes under solvothermal conditions. After cooling to ambient temperature, the product was centrifuged, freeze-dried at -80 °C, lyophilized, and finely powdered to produce carbon nanoparticles.

A phytochemical-mediated reduction technique was used to synthesise zinc oxide nanoparticles by adding 70 mL of carrot extract dropwise to 70 mL of 1 mM $Zn(NO_3)_2$ solution under continuous magnetic stirring. The reaction mixture was agitated for 12 hours, and the solution progressively changed from light yellow to a milky white suspension, which indicated the presence of zinc oxide nanoparticles. The resultant solution was centrifuged at 5000 rpm for 15 minutes, and the white precipitate was rinsed several times with ethanol to eliminate any remaining reactants and contaminants. The purified product was then lyophilised, dried at 60°C for 24 hours, and crushed into a fine nanopowder.

Zinc oxide-carbon nanocomposites were prepared by dispersing carbon nanoparticles and zinc oxide nanoparticles in deionised water at a weight ratio of 2:1, followed by 12 hours of continuous magnetic stirring to ensure a consistent dispersion and a close interfacial interaction between the two nanophases. The solution was centrifuged at 5000 rpm for 15 minutes, and the collected precipitate was lyophilised, vacuum-dried at 60 °C, and coarsely powdered to yield fine black zinc oxide-functionalized carbon nanocomposite powder for further physicochemical characterisation and use.

2.3 Characterisation of Zinc oxide – functionalised Carbon nanocomposites

A Bruker AXS D8 Advance diffractometer with Cu Kα radiation (λ = 1.540598 Å) was used for powder X-ray diffraction (XRD) for structural analysis within a 2θ range of 10°–70°. Making use of a PerkinElmer spectrometer with the KBr pellet technique, Fourier transform infrared (FTIR) spectra were compiled in the 4000–400 cm^{-1} range. Using an EDAX system-equipped scanning electron microscope (HRSEM-EDX, FEI Quanta FEG 200), morphological and elemental characteristics were assessed. The UV-Vis optical absorption spectrum was obtained using a PerkinElmer Lambda 25 spectrometer in the wavelength range of 300-1100 nm.

2.4 Antibacterial Assay

2.4.1 Bacterial strains & Materials used for testing

The antibacterial activity of the nanomaterials was tested against four therapeutically important pathogenic bacterial strains: Pseudomonas aeruginosa, Enterococcus faecalis, methicillin-resistant Staphylococcus aureus (MRSA), and Klebsiella pneumoniae. All bacterial cultures were sourced from the AMR and Nanotherapeutics Laboratory, Department of Pharmacology, Saveetha Dental College and Hospitals, Saveetha Institute of Medical and Technical Sciences (SIMATS), Chennai, India. The agar well diffusion technique was used to test the antibacterial activity of synthetic carbon nanoparticles, zinc oxide nanoparticles, and zinc oxide-functionalized carbon nanocomposites.

2.4.2 Inoculation Preparation

Each bacterial strain was grown in Mueller-Hinton Broth (MHB; HiMedia, Mumbai, India) and incubated for 24 hours at 37 degrees Celsius. To ensure a consistent inoculum for antimicrobial susceptibility testing, the bacterial suspension was adjusted to a turbidity of a 0.5 McFarland standard using sterile normal saline (about 1×10^8 colony-forming units/mL).

2.4.3 Agar Well Diffusion Assay

The antibacterial activity was assessed using the agar well diffusion method. Mueller-Hinton Agar (MHA; HiMedia, Mumbai, India) plates were made and autoclaved at 121 °C for 20 minutes. Following solidification, the agar surface was evenly inoculated with the standardised bacterial solution using a sterile cotton swab. Wells were aseptically punched into the agar with a sterile cork borer. Stock solutions of fabricated nanoparticles were produced in 2% dimethyl sulfoxide (DMSO) at a concentration of 60 mg/mL. Each well received an aliquot of the nanoparticle suspension (20, 40, 60, 80, and 100 µL). Streptomycin (5 µg/well) was employed as the positive control, with 2% DMSO (30 µL) as the negative control. The plates were incubated at 37 °C for 24 hours, and the widths of the zones of inhibition were measured in millimetres to determine the antibacterial activity of synthesised nanomaterials.

3. Results and Discussions

3.1 Structural analysis

The X-Ray Diffraction pattern in **Figure 1A** shows a broad peak for carbon-based nanoparticles, indicating a partially crystalline structure. The XRD pattern shows multiple peak degrees, the most prominent of which are at 18.55°, 42.51°, 43.57°, and 50.22°. While the reflections at 42.51°, 43.57°, and 50.22° correspond to the (100), (101), and (102) planes of disordered graphitic carbon (JCPDS 41-1487) [15], [16], [17], the broader peak at 18.55° is regarded as defectively ordered or amorphous carbon domains with a larger interlayer spacing, as opposed to the optimal (002) reflection of crystalline graphite. This emphasises the turbostratic crystallographic property of the produced carbon-based nanomaterial. The XRD pattern of Zinc oxide nanoparticles from **Figure 1B** showed intense diffraction peaks indexed to the hexagonal wurtzite crystal structure of ZnO. The observed diffraction peaks at approximately 31.8°, 34.4°,

36.3°, 47.5°, and 56.6° corresponded to the (100), (002), (101), (102), and (110) crystallographic planes [18], respectively. The XRD pattern of Zinc oxide functionalised carbon nanocomposites from **Figure 1C** exhibited diffraction peaks corresponding to both graphitic carbon and crystalline ZnO phases, indicating successful nanocomposite formation.

Figure 1 XRD Analysis

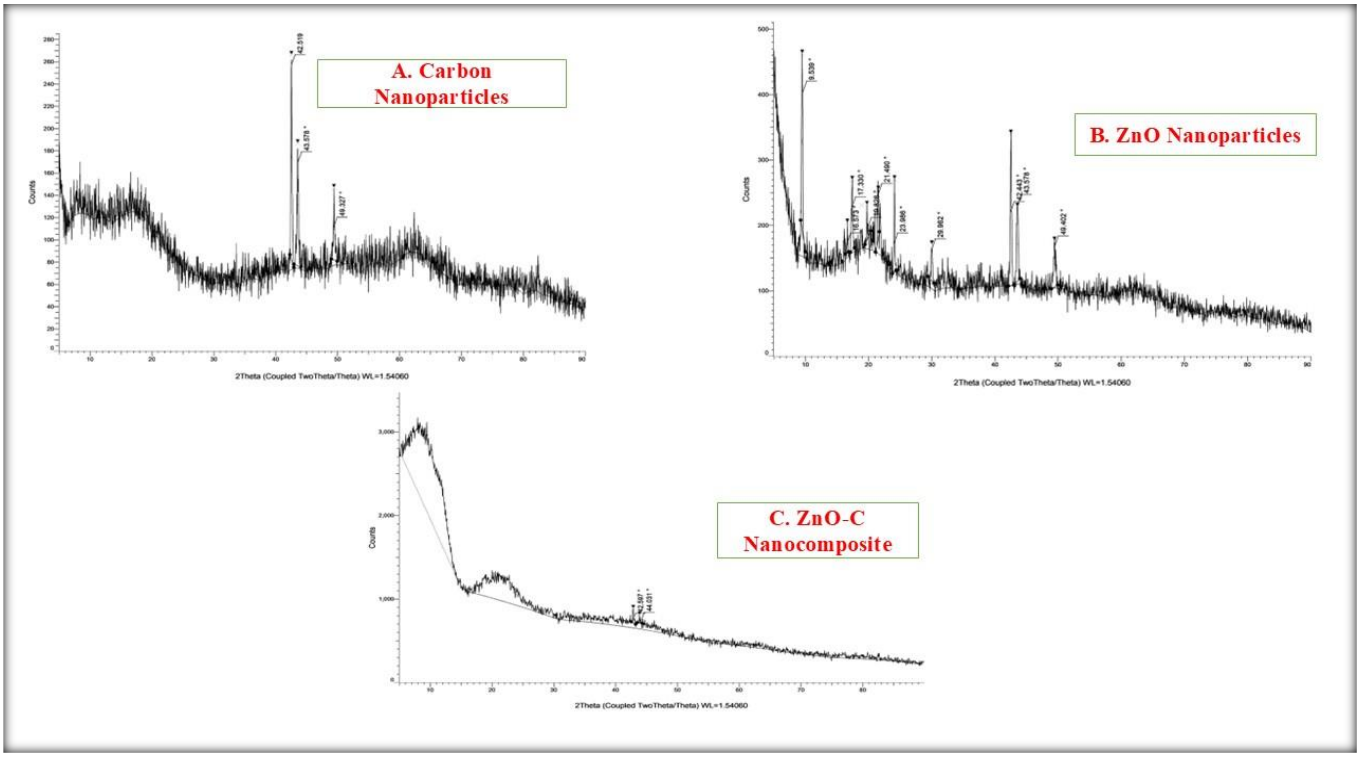

The average crystalline size of the synthesised nanoparticles became apparent by calculating the full width at half maximum (FWHM) and the Debye-Scherrer formula as indicated below:

$D = K\lambda / \beta \cos \theta$ (1)

$D = 0.9\lambda / \beta \cos \theta$ (2)

Where K = 0.9 is the shape factor, β is the line broadening at half the maximum intensity (FWHM) in radians, λ is the X-ray wavelength, and θ is the Bragg angle. According to the Debye—Scherrer equation, the mean particle size values of the as-prepared carbon nanoparticles, zinc oxide nanoparticles and zinc oxide– functionalised carbon nanocomposites were around 48.6 nm, 51.15 nm and 14.11 nm, respectively.

3.2 Functional group analysis

The FTIR spectrum of the Carbon nanoparticles (**Figure 2A**) synthesised using carrot extract, citric acid, PAN indicator, and EDTA exhibited a broad O-H stretching band at 3408 cm^{-1}, signifying hydroxyl groups and adsorbed water [19]. The peak at 2926 cm^{-1} represents C-H stretching [20], whereas the strong band at 1711 cm^{-1} suggests C=O groups [21] from citric acid/EDTA. Peaks with values at 1401, 1199, and 1010

cm^{-1} correspond to $-COO^{-}$, C-O, and C-O-C vibrations [19], indicating the vitality of biomolecules and chelators as surface capping agents. The bands at 774 cm^{-1} indicate C-H bending vibrations [22]. These characteristics confirm the synthesis of carbon nanoparticles with extensive surface functionalization. **Figure 2B** portrays the FTIR spectrum of ZnO nanoparticles, displaying characteristic Zn–O stretching vibrations below 600 cm−1, confirming ZnO formation [23]. From **Figure 2C**, we study the functional groups of the synthesised zinc oxide -functionalised carbon nanocomposite. The absorption band at 3288 cm^{-1} represents hydroxyl groups [24] from phytochemicals in Daucus carota, showing their significance in nanoparticle reduction and stabilisation. The absorption bands between 2873 and 1013 cm^{-1} correspond to C-H, C=O, C=C, and C-O functional groups, indicating the existence of oxygen-containing organic moieties and the carbon matrix's successful synthesis. These functional groups improve the interaction between ZnO nanoparticles and the carbon support. The absorption bands found in the 831-597 cm^{-1} area are due to Zn-O stretching vibrations [23], indicating the synthesis of zinc oxide and its effective integration onto the carbon framework.

Figure 2 FTIR Analysis

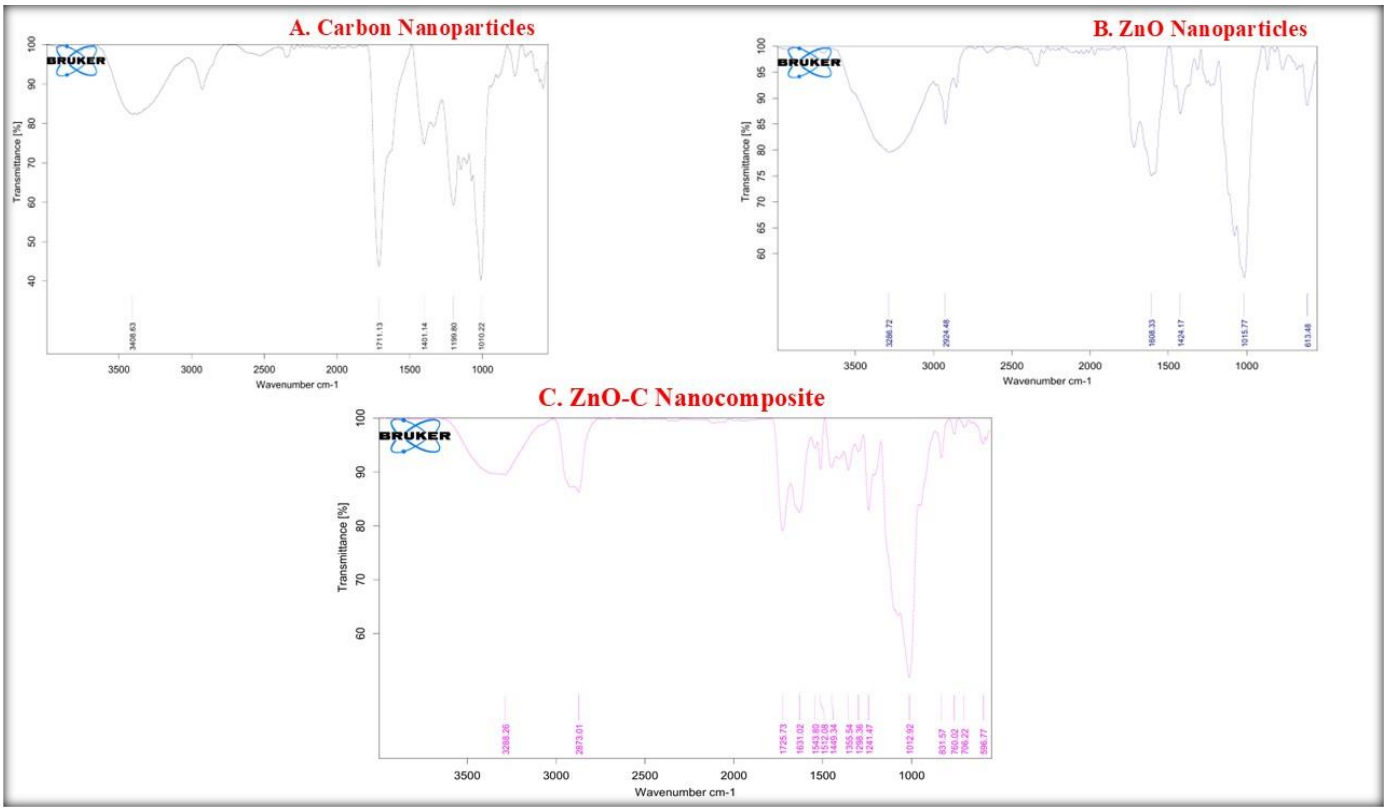

3.3 Morphological analysis

The SEM image of a carbon nanoparticle, as illustrated in **Figure 3A**, indicates mostly compactly arranged spherical particles with a fairly uniform distribution of sizes [13], albeit minor agglomeration is observed. **Figure 3B** displays the SEM image of zinc oxide nanoparticles, exhibiting a quasi-spherical morphology with improved crystallinity [25]. **Figure 3C** exhibits the homogeneous dispersion of ZnO over the carbon matrix, thereby confirming the existence of Zinc oxide – functionalised carbon nanocomposites.

Figure 3 SEM Analysis

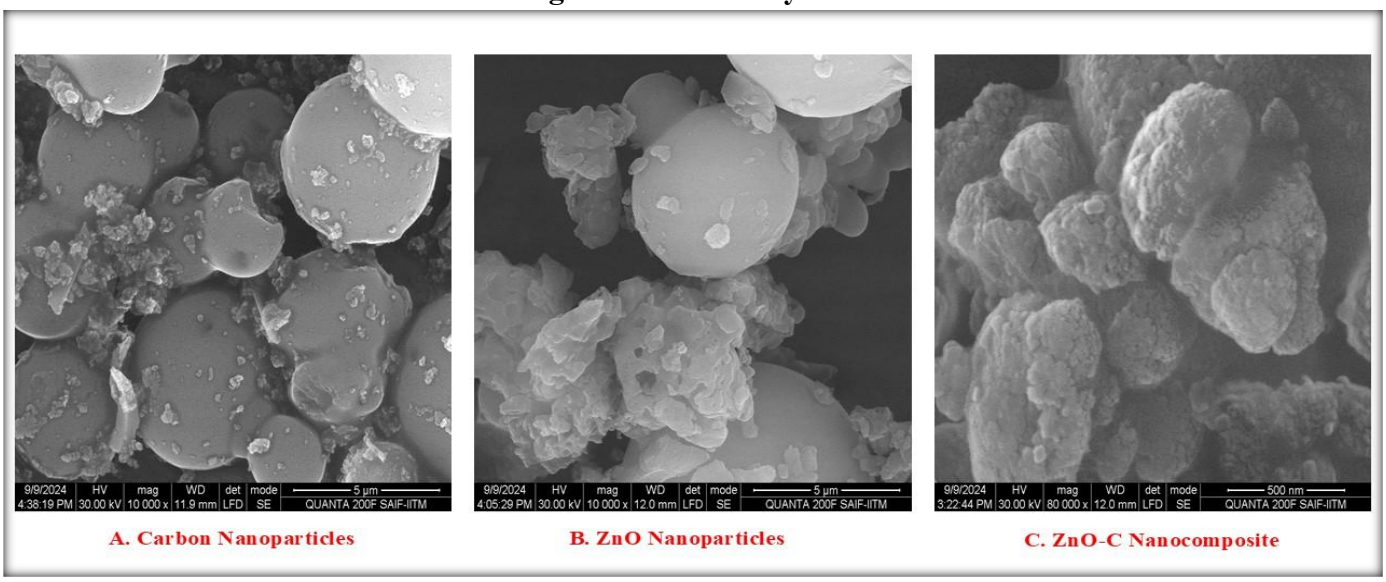

3.4 Elemental analysis

The EDAX of Carbon nanoparticles from **Figure 4A** displays distinctive C and O signals with minimal K traces, showing the synthesis of carrot-mediated carbon nanostructures , whereas **Figure 4B** confirms the elemental presence of Zn and O from zinc oxide nanoparticles [25]. **Figure 4C** confirms the presence of Zn, C, O, and K without detectable impurities, demonstrating successful formation of the nanocomposite system.

Figure 4 EDAX Analysis

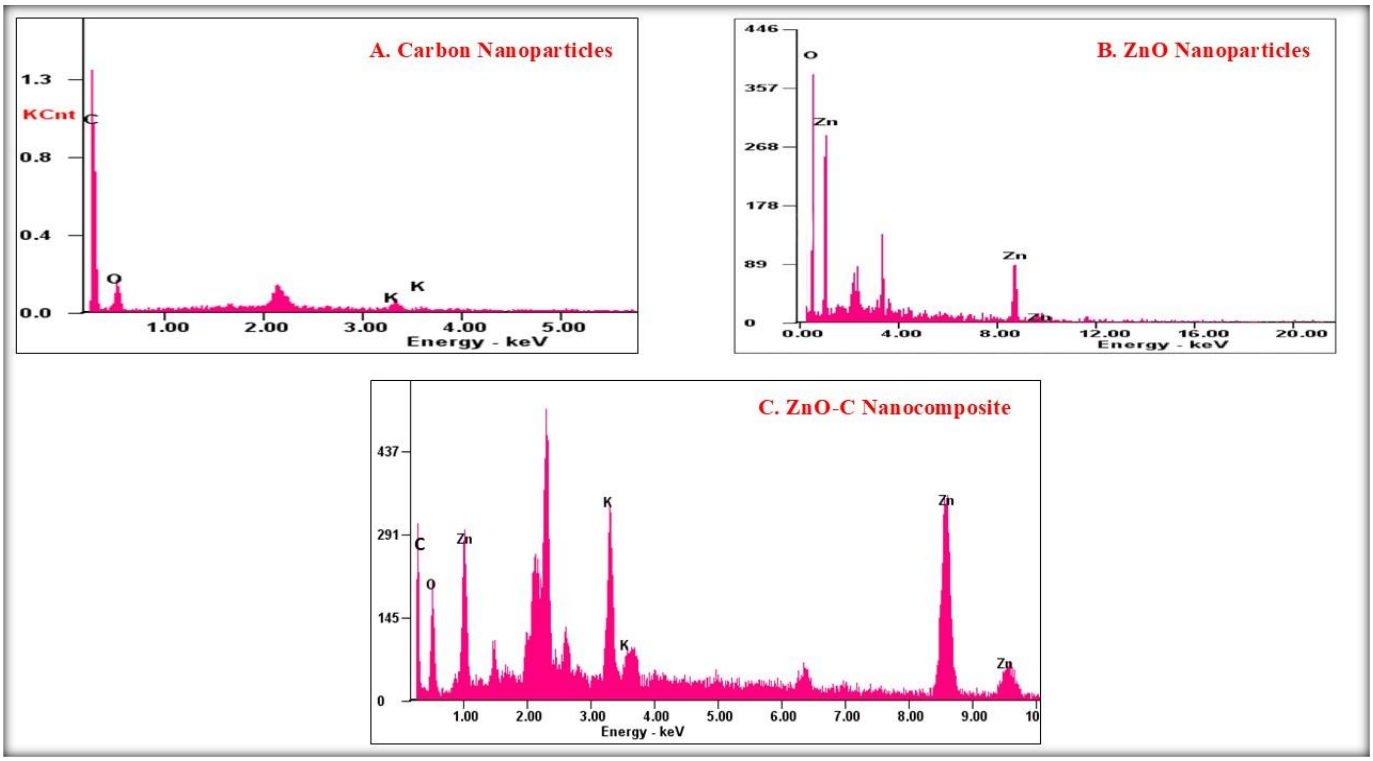

3.5 Optical analysis

The UV pattern of Carbon nanoparticles from **Figure 5A** has a characteristic absorption band at 331 nm, which is related to n-π* electronic transitions of C=O bonds [26]. The use of carrot extract in the mixture optimises optical stability and facilitates nanoparticle formation. Pure ZnO nanoparticles from **Figure 5B** had a significant absorption edge at about 338 nm [27], which corresponds to band-gap excitation. The ZnO-C nanocomposites, as displayed in **Figure 5C,** showed increased visible light absorption and a red shift in the absorption edge. This effect results from interfacial electronic interaction between the ZnO and carbon phases.

Figure 5 UV-Visible Spectroscopic Analysis

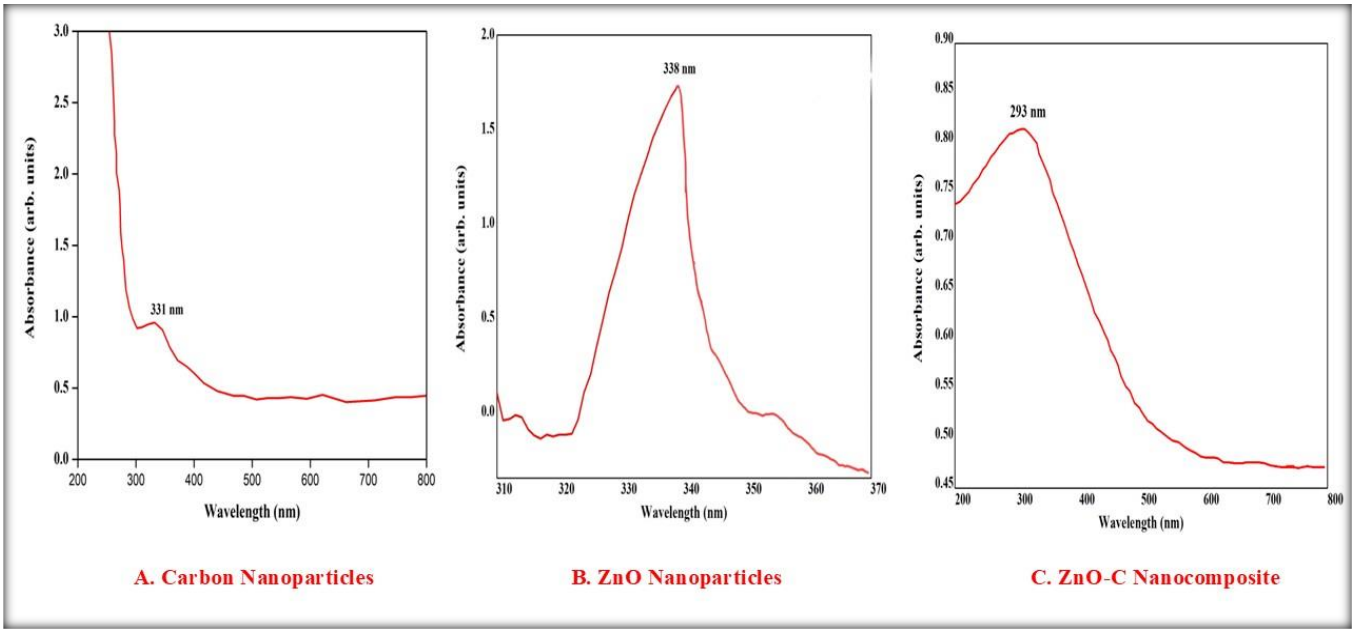

3.6 Antibacterial activity

The antibacterial efficacy of the produced carbon nanoparticles and zinc oxide-functionalized carbon (ZnO-C) nanocomposites was tested against therapeutically relevant Gram-positive and Gram-negative bacterial strains using the agar well diffusion technique. Antimicrobial effectiveness was determined by measuring the width of the inhibitory zones at various nanoparticle concentrations. The results showed concentration-dependent antibacterial activity with different changes in bacterial susceptibility, indicating that ZnO functionalization influences the antimicrobial performance of the carbon matrix. These findings shed light on the potential of ZnO-C nanocomposites as sustainable antimicrobial materials for biomedical applications, notably in the development of methods to battle bacterial infections and antimicrobial resistance.

Green-synthesised carbon nanoparticles demonstrated concentration-dependent antibacterial activity against all four tested bacterial species, as studied from **Figure 6**. Pseudomonas aeruginosa was the most susceptible pathogen, with an inhibition zone ranging from 14 mm at 20 µL to 22 mm at 80 µL.

Methicillin-resistant Staphylococcus aureus (MRSA) exhibited strong antibacterial sensitivity, with inhibition zones ranging from 15 mm to 18 mm, while Enterococcus faecalis showed moderate inhibition (13-17 mm). Klebsiella pneumoniae was comparatively less susceptible, producing inhibition zones of 11-18 mm across the tested concentrations. The steady rise in inhibitory zones with increasing nanoparticle concentration suggests increased antibacterial activity [28]. The observed activity is attributable to the carbon nanoparticles' large surface area, the presence of oxygen-containing surface functional groups, and phytochemical residues from Daucus carota, all of which contribute to bacterial membrane breakdown and oxidative stress.

Figure 6 Antibacterial activity of carbon nanoparticles

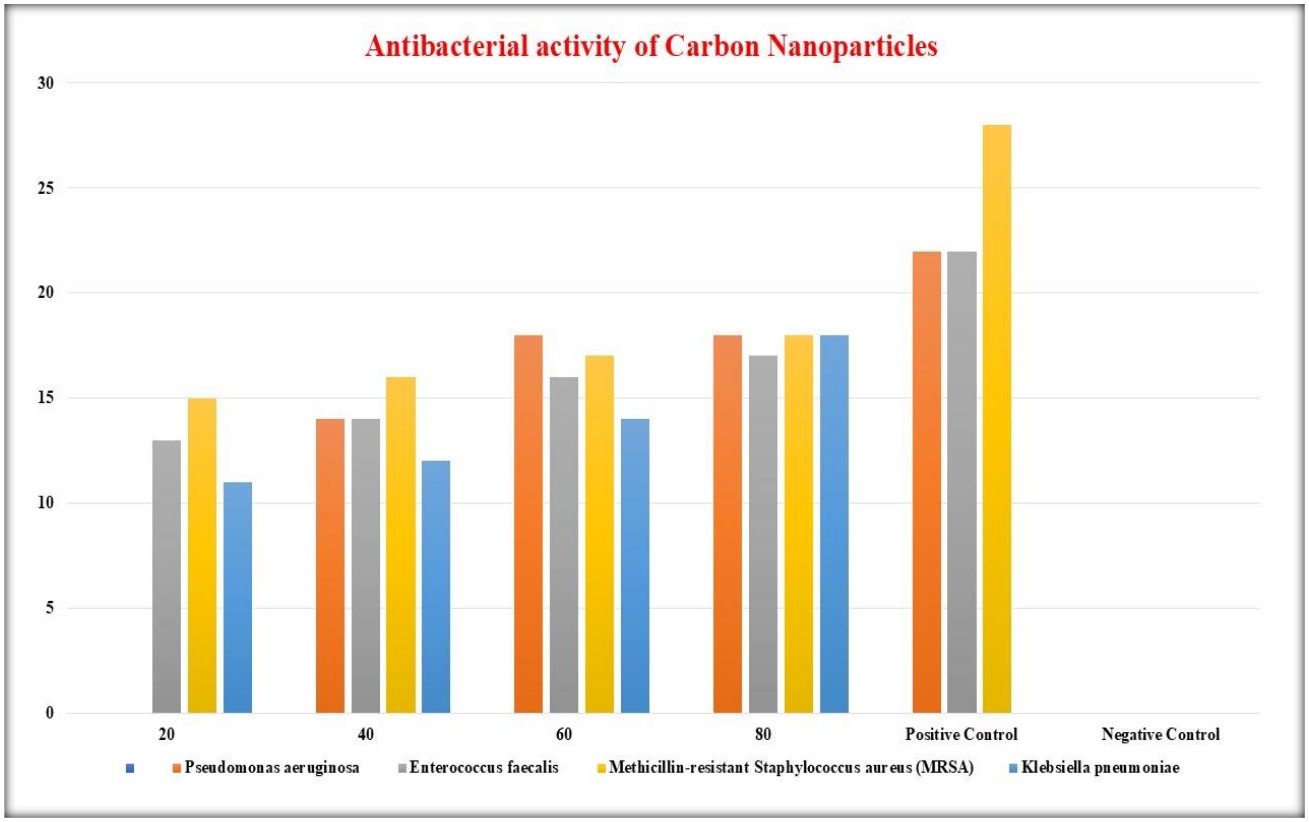

The antibacterial activity of synthesised zinc oxide-functionalized carbon (ZnO-C) nanocomposites differed significantly amongst the studied bacterial strains, showing selective antimicrobial effectiveness; this is shown in **Figure 7**. Pseudomonas aeruginosa showed the highest sensitivity to the nanocomposite, with a 24 mm zone of inhibition at 20 µL, indicating its remarkable bactericidal ability against these opportunistic Gram-negative bacteria. MRSA inhibition zones increased from 11 mm (20 µL) to 12 mm (40 µL), 13 mm (60 µL), and 14 mm (80 µL), indicating improved antibacterial efficacy with increasing nanocomposite concentration. However, the activity was lower than that of streptomycin, the positive control that formed a 25 mm inhibitory zone. There was no visible antibacterial activity against Enterococcus faecalis or Klebsiella pneumoniae at the tested doses, but the positive control exhibited a 22 mm inhibition zone against Enterococcus faecalis, confirming the assay's validity.

Figure 7 Antibacterial activity of Zinc oxide – Carbon nanocomposite

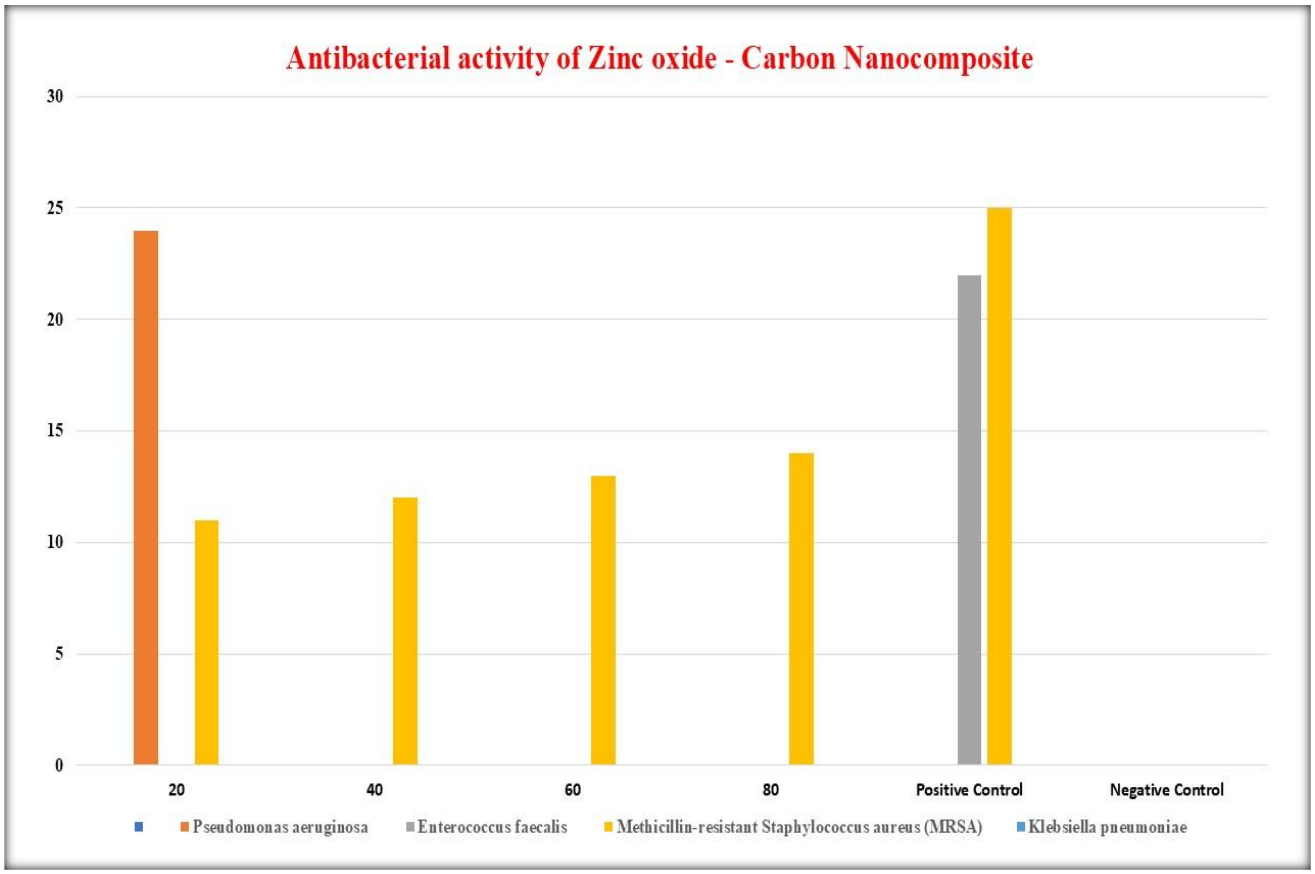

Therefore, we observe that the carbon nanoparticles exhibited broader antibacterial activity against all tested bacterial strains, whereas zinc oxide-functionalized carbon (ZnO-C) nanocomposites demonstrated enhanced antibacterial efficacy specifically against Pseudomonas aeruginosa, indicating that ZnO functionalization improves pathogen-specific activity while reducing the carbon nanoparticles' broad-spectrum antimicrobial effect.

4. Conclusion

Zinc oxide-functionalized carbon (ZnO–C) nanocomposites were effectively created employing a green solvothermal approach with Daucus carota extract acting as a natural reducing and stabilizing agent. Characterization studies verified the successful development of the zinc oxide – functionalised carbon nanocomposite with the required structural and functional properties. With the greatest inhibition against Pseudomonas aeruginosa (24 mm) and moderate activity against MRSA (11–14 mm), the ZnO–C nanocomposites demonstrated selective antibacterial action, whereas Enterococcus faecalis and Klebsiella pneumoniae showed very little susceptibility. ZnO nanoparticles and the carbon matrix work together to produce reactive oxygen species, liberate Zn2+ ions, and promote nanoparticle dispersion, all of which contribute to the improved antibacterial activity. These results demonstrate the promise of green-

synthesised ZnO–C nanocomposites as environmentally friendly antibacterial materials for the creation of cutting-edge biomedical and healthcare applications.

5. Acknowledgements

The authors express their gratitude to Dr Saravanan Muthupandian, Ex-Professor, Saveetha Dental College, Saveetha Institute of Medical and Technical Sciences, Chennai, for providing us with the required facilities to carry out this research work. We also extend our thanks to Shalini J and Geetha Sravanthy P for their assistance and support during the experimental phase of this work.

References

1. S. Kumar, V. Kumar, C. S. Pathak, A. Mishra, M. K. Bansal, and R. S. Baghel, “A comprehensive review on ZnO wide-bandgap semiconductors: Materials engineering, properties, and emerging applications,” Results Mater., vol. 30, no. January, pp. 1–13, 2026, doi: 10.1016/j.rinma.2026.100929.
2. R. Emram, R. V. Sionov, V. Gutkin, A. Wilensky, D. Steinberg, and R. Assad, “Mechanism of Action of Zinc Oxide Nanoparticles as an Antibacterial Agent Against Streptococcus mutans,” Biomolecules, vol. 15, no. 12, pp. 1–23, 2025, doi: 10.3390/biom15121660.
3. G. Awasthi et al., “Green electrochemical synthesis of ZnO-graphene composite nanopowder and its improved antimicrobial properties,” Next Nanotechnol., vol. 7, no. December 2024, pp. 1–6, 2025, doi: 10.1016/j.nxnano.2025.100183.
4. Z. Villagrán et al., “Plant-Based Extracts as Reducing, Capping, and Stabilizing Agents for the Green Synthesis of Inorganic Nanoparticles,” Resources, vol. 13, no. 6, 2024, doi: 10.3390/resources13060070.
5. A. Halder, G. R. Mohan, S. Matheshwaran, and S. K. Jha, “Green synthesis of neem (Azadirachta indica) functionalized zinc oxide with enhanced antimicrobial properties,” Next Mater., vol. 8, no. April, 2025, doi: 10.1016/j.nxmate.2025.100725.
6. S. Singh and B. Jain, “Green Synthesis of Zinc Oxide Nanoparticles Using Aloe Vera: a Study on Optical Properties and Photocatalytic Activity,” Orcid:, no. February, 2024.
7. A. Ben Amor et al., “Synthesis of spherical carbon nanoparticles from orange peel and their surface modification with chitosan: Evaluation of optical properties, biocompatibility, antioxidant and anti-hemolytic activity,” Biomass Convers. Biorefinery, vol. 15, no. 7, pp. 11345–11358, 2025, doi:
8. C. J. Jeong et al., “Fluorescent carbon nanoparticles derived from natural materials of mango fruit for bio-imaging probes,” Nanoscale, vol. 6, no. 24, pp. 15196–15202, 2014, doi: 10.1039/c4nr04805a.
9. P. D. Barata, A. I. Costa, S. Martins, M. C. Semedo, B. G. Antunes, and J. V. Prata, “One-Pot Microwave-Assisted Synthesis of Fluorescent Carbon Dots from Tomato Industry Residues with Antioxidant and Antibacterial Activities,” Biomass (Switzerland), vol. 5, no. 2, pp. 1–19, 2025, doi: 10.3390/biomass5020035.
10. M. Poshtkar, A. Rezazadeh, M. Haeili, Z. Ghasempour, and A. Ehsani, “P-doped carbon quantum dots from potato starch as antimicrobial materials for food applications,” Lwt, vol. 232, no. August, 2025, doi: 10.1016/j.lwt.2025.118399.

11. M. Mantiniotou, V. Athanasiadis, D. Kalompatsios, and S. I. Lalas, “Optimization of Carotenoids and Other Antioxidant Compounds Extraction from Carrot Peels Using Response Surface Methodology,” Biomass (Switzerland), vol. 5, no. 1, 2025, doi: 10.3390/biomass5010003.
12. I. A. Baba et al., “Influence of plant-derived extracts on the synthesis, physicochemical properties, and applications of metal and metal oxide nanoparticles,” Hybrid Adv., vol. 13, no. April, 2026, doi: 10.1016/j.hybadv.2026.100666.
13. S. L. D’souza, S. S. Chettiar, J. R. Koduru, and S. K. Kailasa, “Synthesis of fluorescent carbon dots using Daucus carota subsp. sativus roots for mitomycin drug delivery,” Optik (Stuttg)., vol. 158, pp. 893–900, 2018, doi: 10.1016/j.ijleo.2017.12.200.
14. F. Yan, Y. Jiang, X. Sun, J. Wei, L. Chen, and Y. Zhang, “Multicolor carbon dots with concentration-tunable fluorescence and solvent-affected aggregation states for white light-emitting diodes,” Nano Res., vol. 13, no. 1, pp. 52–60, Jan. 2020, doi: 10.1007/s12274-019-2569-3.
15. Y. A. Saber, M. Hamed, S. Emara, F. R. Mansour, M. Locatelli, and N. Ibrahim, “Garlic peel-based carbon quantum dots as a sustainable alternative for the sensitive and green spectrofluorometric quantification of molnupiravir in pharmaceutical capsules,” Heliyon, vol. 10, no. 23, 2024, doi: 10.1016/j.heliyon.2024.e40661.
16. H. A. Mohammed et al., “Sustainable hydrothermal synthesis of ultrasmall carbon quantum dots from drinking coffee and their impact on optoelectronic properties of the methyl cellulose biopolymer,” Mater. Adv., 2026, doi: 10.1039/d6ma00178e.
17. A. F. Shaikh, M. S. Tamboli, R. H. Patil, A. Bhan, J. D. Ambekar, and B. B. Kale, “Bioinspired Carbon Quantum Dots: An Antibiofilm Agents,” J. Nanosci. Nanotechnol., vol. 19, no. 4, pp. 2339–2345, 2018, doi: 10.1166/jnn.2019.16537.
18. T. Khao, R. O. Gembo, S. Odisitse, and C. K. King’ondu, “Fabrication of ZnO nanoparticles using marula (Sclerocarya birrea) leaf extract for catalytic degradation of rhodamine 6 G and methylene blue dyes under UV light irradiation,” Next Mater., vol. 7, no. August 2024, 2025, doi: 10.1016/j.nxmate.2024.100366.
19. N. Hussain, S. Alwan, H. Alshamsi, and I. Sahib, “Green Synthesis of S- A nd N-Codoped Carbon Nanospheres and Application as Adsorbent of Pb (II) from Aqueous Solution,” Int. J. Chem. Eng., vol. 2020, 2020, doi: 10.1155/2020/9068358.
20. J. Shen, S. Shang, X. Chen, D. Wang, and Y. Cai, “Facile synthesis of fluorescence carbon dots from sweet potato for Fe3 + sensing and cell imaging,” Mater. Sci. Eng. C, vol. 76, pp. 856–864, Jul. 2017, doi: 10.1016/j.msec.2017.03.178.
21. J. C. Kung, I. T. Tseng, C. S. Chien, S. H. Lin, C. C. Wang, and C. J. Shih, “Microwave assisted synthesis of negative-charge carbon dots with potential antibacterial activity against multi-drug resistant bacteria,” RSC Adv., vol. 10, no. 67, pp. 41202–41208, 2020, doi: 10.1039/d0ra07106d.
22. S. A. Akbar et al., “Fluorescent carbon quantum dots from Syzygium aromaticum as a selective sensor for Fe3+ and Cd2+ detection in aqueous solution,” Case Stud. Chem. Environ. Eng., vol. 11, no. February, p. 101166, 2025, doi: 10.1016/j.cscee.2025.101166.
23. A. Molla et al., “Green synthesis of ZnO nanoparticles using Citrus sinensis peel: optimizing volume ratios for enhanced antibacterial and banana preservation activities,” BMC Biotechnol., vol. 26, no. 1, 2026, doi: 10.1186/s12896-026-01145-x.
24. V. V Deepa R, Muthuraj D, Kumar E, “Microwave assisted synthesis of Zinc oxide nanoparticles,” J. Nanosci. Technol., vol. 5, no. 1, pp. 640–641, 2019, doi: 10.1016/j.mspro.2015.11.101.

25. M. Mahajan et al., “Surface-modified ZnO nanoparticles for enhanced environmental and biomedical performance,” Hybrid Adv., vol. 8, no. November 2024, 2025, doi: 10.1016/j.hybadv.2024.100342.
26. P. Jana and A. Dev, “Green Synthesis of Fluorescent Carbon Dots through Solvothermal Treatment of Buchnania lanzan Leaf Extract,” p. 59, 2022, doi: 10.3390/ecsoc-25-11648.
27. J. Ashwini, T. R. Aswathy, A. B. Rahul, G. M. Thara, and A. S. Nair, “Synthesis and characterization of zinc oxide nanoparticles using acacia caesia bark extract and its photocatalytic and antimicrobial activities,” Catalysts, vol. 11, no. 12, 2021, doi: 10.3390/catal11121507.
28. T. Ananda, A. Modi, V. Managuli, and C. Mukhopadhyay, “Antimicrobial Property of Silver Nanoparticles: Effects of Concentration and Temperature on Bacterial Isolates,” J. Pure Appl. Microbiol., vol. 17, no. 2, pp. 1118–1127, 2023, doi: 10.22207/JPAM.17.2.42.